Available online at www.sciencedirect.com
ScienceDirect
Mathematics and Computers in Simulation 80 (2010) 2109–2114
MATHEMATICS AND COMPUTERS IN SIMULATION
www.elsevier.com/locate/matcom

The importance of Monte Carlo simulations in modeling detectors for Nuclear Medicine

Nico Lanconelli

Dipartimento di Fisica, Alma Mater Studiorum, University of Bologna, Viale Berti-Pichat 6/2, I-40127 Bologna, Italy

Received 27 September 2007; received in revised form 6 April 2010; accepted 11 April 2010
Available online 22 April 2010

Abstract

Nowadays, Monte Carlo techniques are very common for the development of Nuclear Medicine systems. Simulations can be very helpful for the optimization of SPECT and PET cameras, and for investigating the importance of several physical effects involved in image formation. In this paper, a simulation study for evaluating various aspects inuencing image formation in detectors for Nuclear Medicine is presented. To this end, the EGSnrc Monte Carlo code has been used, which transports photons and electrons in any material and handling various physical phenomena. Here, some detector systems are simulated, consisting of a parallel-hole collimator and a pixellated scintillator. Various effects are investigated, such as electron transport, uorescence photons, collimator septa penetration. Results are evaluated by means of energy spectra, photon uxes, uniformity of response, SNR and spatial resolution.

Keywords: Monte Carlo; Particle transport; Nuclear Medicine; Detector modeling

1. Introduction

Monte Carlo techniques are becoming very popular for transporting particles [1,9] and for the development of Nuclear Medicine apparatus [12]. Their usefulness is noticeable both in the optimization of the design of SPECT and PET cameras [6,10,13] and in the investigation of the effects which influence the behavior of a device. Monte Carlo methods offer a possibility of gaining an understanding of the physics that forms images and provide help in developing procedures to improve them. Phenomena like Rayleigh or Compton scattering, fluorescence photons, electron transport can be isolated and their effects can be analyzed each one independently of the others.

The aim of this paper is to perform Monte Carlo simulations to examine the importance of various aspects influencing image formation in detectors for Nuclear Medicine. In this way, it is possible to evaluate which approximations can be done in Monte Carlo simulations without affecting the outcomes. To this end we utilize EGS code in one of its latest versions, named EGSnrc [7]: this code handles a lot of physical phenomena and incorporates cross-sections of many materials (potentially any material can be simulated, if we know its composition). We developed some user-written routines, for the simulation of parallel collimators with hexagonal or square holes and pixellated detectors with dead zone included [2]: the routines have been tested for the design of various detection systems for Nuclear Medicine [3–5,8,11]. Other issues that will be explored concerns the consequences of the mismatching between the lattices of hexagonal collimators and pixellated detectors. Results are evaluated

E-mail address: nico.lanconelli@unibo.it.

0378-4754/$36.00
doi:10.1016/j.matcom.2010.04.004

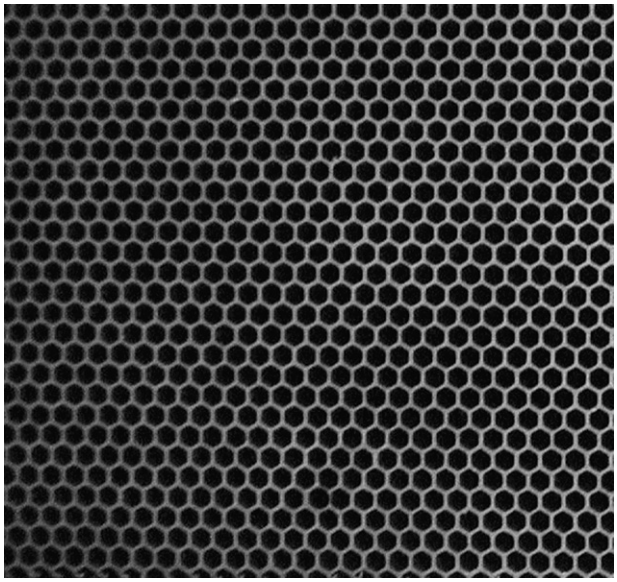

Fig. 1. Picture of the front side of a parallel collimator with hexagonal holes in hexagonal lattice.

in terms of energy spectra, photon fluxes, uniformity of response, SNR and spatial resolution of the simulated systems.

2. Methods

A typical scintillation camera for imaging in the Nuclear Medicine field consists of two main components: a collimator and a scintillation crystal. Collimators permit the selection of the acceptance angle of the photons impinging the detector. Parallel collimators are usually made of lead or tungsten and contain hundreds (or thousands) of parallel holes through which photons are allowed to pass. Holes can have different shapes: round, squares, and hexagonal are the most common. Fig. 1 shows a picture of the front side of a typical parallel collimator with hexagonal holes.

Photons which pass the collimator reach the scintillation crystal, where each interaction produces light photons. Usually it consists of a scintillator material, such as Sodium Iodide doped with Thallium (NaI(Tl)). The scintillator can be a planar single crystal or can be composed of several small elements (pixellated detector).

The first issue investigated in this paper is the assessment of the imprecision in the simulation of parallel hole collimators. There are different approaches for their simulation: on one side we can treat them as merely "geometric" barriers to the particle transport and thus discard the particles as soon as they impinge on the collimator septa [6]. On the other hand, we can simulate the collimator taking into account all the physical aspects we can handle (*e.g.* septa penetration, scattering, fluorescence photons, etc.). In order to estimate the importance of these effects we performed different simulations: in the first one, named "geometric", we discard the particles as soon they impinge on the lead septa, in the "full" simulation we use all the phenomena EGS allows us to simulate; other simulations are achieved from the "full" one, by neglecting each time one effect (electron transport, Compton and Rayleigh scattering). For each simulation we calculated the number of particles exiting from the collimator and their spectra. We simulated a 140 keV point source in air, located at various distances (ranging from 2 cm to 40 cm) from the collimator; the features of the simulated collimators are shown in Table 1.

Table 1
Features of the two simulated collimators: High-Sensitivity (HS) and General Purpose (GP).

Collimator	Hole diameter [mm]	Thickness [mm]	Septa [mm]
HS	3.0	30	0.2
GP	1.5	22	0.2

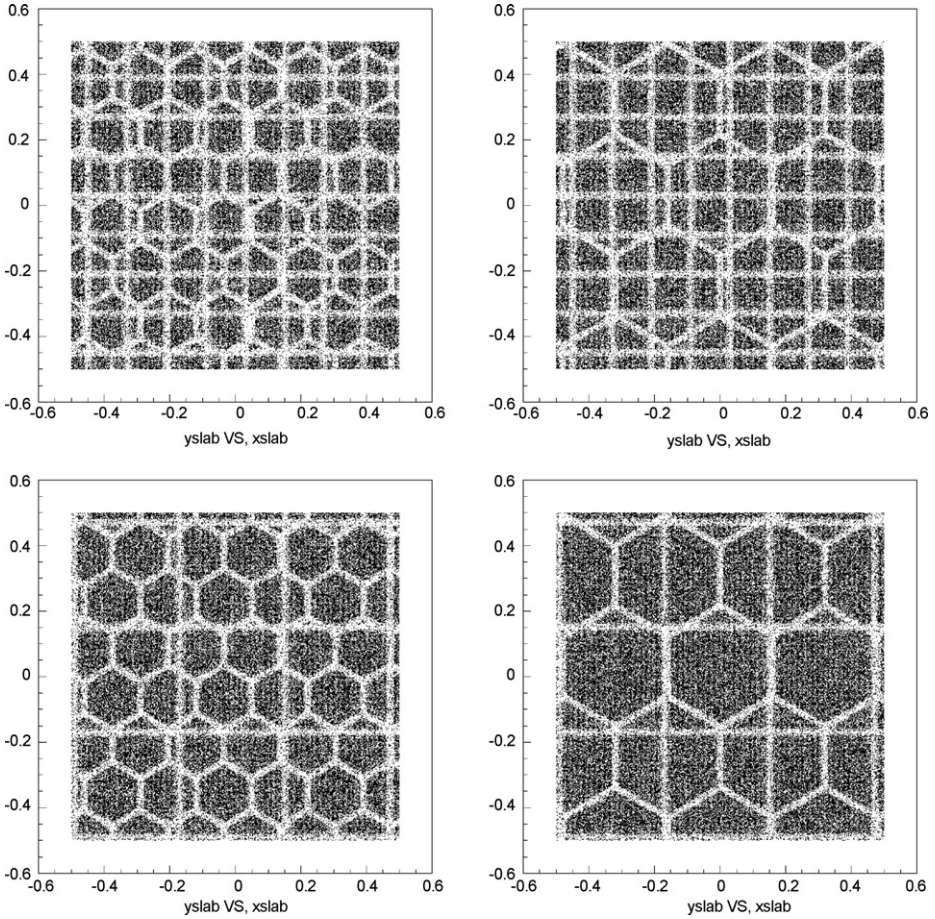

Fig. 2. Scatter plot of the spatial distribution for detected photons coming from a parallel flood irradiation. Two different pixel sizes (1 mm and 3 mm with 0.2 mm dead zone) and two different collimators (HS and GP) are simulated. Results for the GP and HS collimator are shown on the left and on the right, respectively. Results for the 1 mm and 3 mm pixels are shown on the top and on the bottom, respectively.

The second issue examined is the variation in the uniformity response of a pixellated detector, caused by the mismatch between the hexagonal collimator lattice and the square pixel lattice (including dead zones). We simulated a parallel flood irradiation of 140 keV photons (some examples of the final photon planar coordinates are shown in Fig. 2).

Two collimators are considered (HS and GP in Table 1) and two different 1/2 in. thick NaI crystals: the first one with 1 mm × 1 mm pixels and the second one with 3 mm × 3 mm pixels (the dead zone is equal to 0.2 mm in both cases). The distribution of the detected photons for each pixel is then analyzed, in order to find out the fluctuations due to the mismatching.

3. Results and discussion

As first result, we can note that from our simulations it turned out that the electrons transport gives a negligible contribution to the simulation outcomes, whereas the execution time increases significantly when we activate this effect. EGSnrc uses a Class II Condensed History scheme for the simulation of electron transport. We used the default electron transport method available with EGSnrc, called PRESTA-II, which has various improvements with respect to techniques implemented in EGS4, especially in boundaries crossing and multiple scattering theory. More details about the description of the electron transport implemented in EGSnrc can be found in [7]. We neglect the electrons transport by forcing the electrons to deposit all their energy, as soon as they have been generated. In fact, for all the simulations considered in this paper, results do not change in an appreciable way, whether we decided to transport electrons or not.

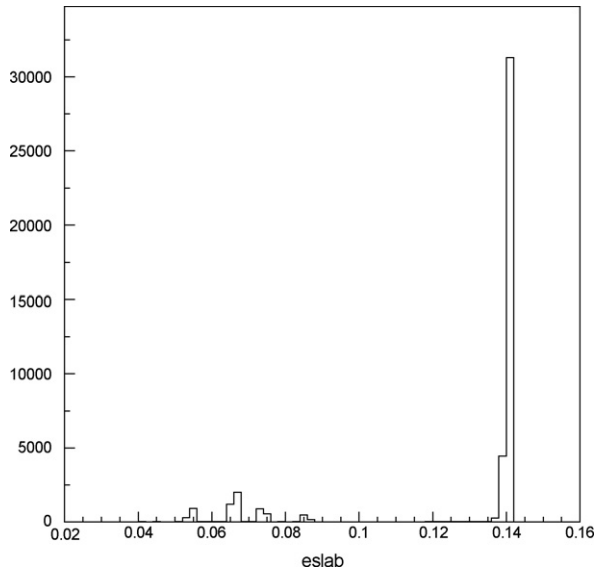

Fig. 3. Example of an energy spectrum of the detected photons. Energies are plotted in MeV. The 140 keV peak is relative to the monochromatic photon source, whereas the peaks located into the 70–90 keV are due to the fluorescence photons emitted by the lead collimator.

In contrast, the execution time ranges from 2 times to about 10 times the time needed for the simulation without the transport of electrons, according to which materials are present in the simulation. Thus, all the results we will present are obtained from simulations where the transport of the electrons was not used.

The fluorescence photons can be a conspicuous fraction of the detected events, according to the simulated scenario. Indeed, we found out that they ranges from about 10% to about 20% of the total number of particles reaching the detector, for a 140 keV source and lead collimators. The amount of fluorescence photons depends both from the energy of the sources and from the amount of background material, since photons can scatter here, thus reaching the collimator with a lower energy. Fig. 3 shows an example of the energy spectra for the detected photons. We can note that some secondary peaks are present, together with the primary peak due to the monochromatic source. In particular, a couple of peaks in the range 70–90 keV are due to the fluorescence photons emitted by the lead collimator.

Figs. 4 and 5 show the simulated results for the sensitivity and the spatial resolution of the GP collimator, respectively. Results were achieved by simulating a point source in air positioned at different distances from the collimator. The spatial resolution was estimated as the Full-Width at Half Maximum (FWHM) of the collimator response. Three different simulations are illustrated: the first one (full simulation) considers all the physical effects available within EGS, the second one considers only primary photons, whereas in the third simulation the collimator is simulated as a "geometric" obstacle (*i.e.* each particle is discarded as soon as it impinges the lead of the collimator).

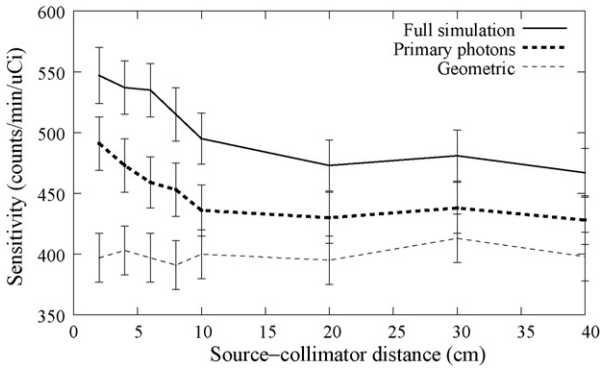

Fig. 4. Sensitivity of the GP collimator as a function of the collimator-to-source distance. Three different results are considered: with all the physical effects simulated (full simulation), only for primary photons, and considering the collimator as a "geometric" obstacle.

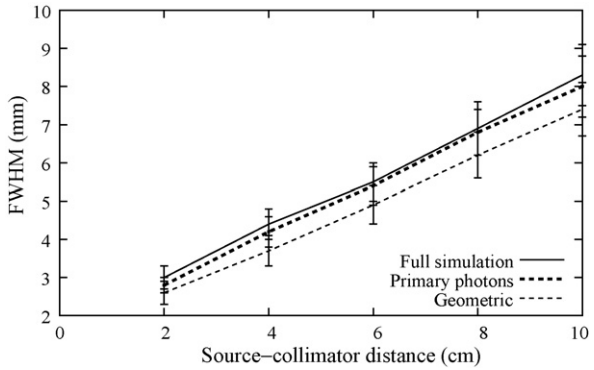

Fig. 5. Spatial resolution of the GP collimator as a function of the collimator-to-source distance. Three different results are considered: with all the physical effects simulated (full simulation), only for primary photons, and considering the collimator as a "geometric" obstacle.

Table 2
Mean value, minimum and maximum for the pixels of the simulated cameras irradiated with a parallel flood source.

Simulated configuration	Average pixel value	Minimum	Maximum
Coll. HS—1 mm × 1 mm pixel	470 ± 80	300	625
Coll. HS—3 mm × 3 mm pixel	4310 ± 60	4180	4430
Coll. GP—1 mm × 1 mm pixel	440 ± 50	338	603
Coll. GP—3 mm × 3 mm pixel	4040 ± 70	3899	4180

It is worth noting that there is a substantial difference in the collimator sensitivity, according to the considered simulation. In particular, the sensitivity is basically independent from the distance, if we consider the collimator as a merely geometric obstacle. On the other hand, the efficiency increases for sources located near the collimator, for simulations which include the physical effects. As expected, the full simulation provides the maximum sensitivity, since it allows photons to reach the detector after having undergone any physical effect. If we neglect scattering or other effects, we get a smaller sensitivity, since in this case we basically consider only primary photons. The geometric sensitivity is further reduced, since in this case we also reject photons which reach the detector after having penetrated the collimator septa. This disparity can be up to 30% and is much more clear for sources located near the collimator: indeed septa penetration plays here a more important role, whereas for photons coming from greater distances this effect is less significant for geometric reasons. The spatial resolution of the collimator seems not to be influenced by photons scattered within the collimator. Conversely, the collimator shows a better spatial resolution, when we simulated it in a geometric way. Again, this difference is due to photons which penetrate collimator septa, giving rise to an increase of the spatial resolution.

Finally, we investigated the presence of a non-uniform response of the camera, caused by the mismatching between the collimator and the pixellated detector lattices. Fig. 2 shows some scatter plots of the four different simulated configurations. In Table 2 the distribution of the pixel values is shown, for the same four conditions.

It turns out that for the 3 mm × 3 mm pixel the response of the camera is almost uniform with both the collimators (the standard deviation is of the same order of magnitude of the root of the mean pixel value). In case of the 1 mm × 1 mm pixel, a non-uniformity is present, caused by the mismatching of the collimator-pixel lattices; this effect is more evident for the collimator with larger holes (collimator HS). A similar behaviour can be observed by estimating the fluctuations in the Signal-to-Noise ratio (SNR) between a small tumor and a flat background, when we change the location of the tumor, with respect to the camera. We simulated a spherical tumor (with a diameter equal to 5 mm), and a camera with GP (or HS) collimator and a pixellated detector with 2 mm pixels and 0.2 mm dead zone. Tumor was positioned at various locations, and for each position the SNR of the tumor over the background is estimated. It turned out that for the GP collimator the maximum fluctuation observed for the SNR value is about 12%, whereas for the HS collimator it can go up to about 20%. All these information are extremely useful, in order to chose the better collimator-pixellated detector configuration.

References

[1] S. Agosteo, C. Birattari, A. Foglio Para, M. Silari, L. Ulrici, FLUKA simulations and measurements for a dump for a 250 GeV/c hadron beam, Math. Comput. Simul. 55 (2001) 3–14.
[2] D. Bollini, R. Campanini, M. Gombia, N. Lanconelli, A. Riccardi, A modular description of the geometry in Monte Carlo modeling studies for Nuclear Medicine, Int. J. Mod. Phys. C 13 (4) (2002) 465–476.
[3] M.N. Cinti, R. Pani, F. Garibaldi, R. Pellegrini, M. Betti, N. Lanconelli, A. Riccardi, R. Campanini, G. Zavattini, G. Di Domenico, A. Del Guerra, N. Belcari, W. Bencivelli, A. Motta, A. Vaiano, I.N. Wienberg, Custom breast phantom for an accurate tumor SNR analysis, IEEE Trans. Nucl. Sci. 51 (1) (2004) 198–204.
[4] M.N. Cinti, R. Pani, R. Pellegrini, C. Bonifazzi, R. Scafé, G. De Vincentis, F. Garibaldi, F. Cusanno, R. Campanini, N. Lanconelli, A. Riccardi, Tumor SNR analysis in scintimammography by dedicated high contrast imager, IEEE Trans. Nucl. Sci. 160 (5) (2001) 1618–1623.
[5] M.N. Cinti, R. Scafé, R. Pellegrini, C. Trotta, P. Bennati, S. Ridolfi, N. Lanconelli, L. Montani, F. Cusanno, F. Garibaldi, J. Telfer, R. Pani, CsI(Tl) micro-pixel scintillation array for ultra-high resolution gamma-ray imaging, IEEE Trans. Nucl. Sci. 54 (2007) 469–474.
[6] G.J. Gruber, W.W. Moses, S.E. Derenzo, Monte Carlo simulation of breast tumor imaging properties with compact, discrete gamma camera, IEEE Trans. Nucl. Sci. 46 (6) (1999) 2119–2123.
[7] I. Kawrakow, Accurate condensed history Monte Carlo simulation of electron transport. I. EGSnrc, the new version, Med. Phys. 27 (4) (2000) 485–498.
[8] A. Motta, S. Righi, A. Del Guerra, N. Belcari, A. Vaiano, G. Di Domenico, G. Zavattini, R. Campanini, N. Lanconelli, A. Riccardi, A full Monte Carlo simulation of the YAP-PEM prototype for breast tumor detection, Nucl. Instrum. Meth. A 527 (2004) 201–205.
[9] H.E. Nilsson, E. Dubaric, M. Hjelm, U. Englund, Monte Carlo simulation of the transient response of single photon absorption in X-ray pixel detectors, Math. Comput. Simul. 62 (2003) 471–478.
[10] C. Ross Schmidtlein, A.S. Kirov, S.A. Nehmeh, Y.E. Erdi, J.L. Humm, H.I. Arnolds, L.M. Bidaut, A. Ganin, C.W. Stearns, D.L. McDaniel, K.A. Hamacher, Validation of GATE Monte Carlo simulations of the GE Advance/Discovery LS PET scanners, Med. Phys. 33 (1) (2006) 198–208.
[11] S. Vecchio, N. Belcari, P. Bennati, M. Camarda, R. Campanini, M.N. Cinti, A. Del Guerra, E. Iampieri, N. Lanconelli, R. Pani, L. Spontoni, A single photon emission computer tomograph for breast cancer imaging Imaging, Nucl. Instrum. Meth. A 581 (2007) 84–87.
[12] H. Zaidi, Relevance of accurate Monte Carlo modeling in Nuclear Medicine imaging, Med. Phys. 26 (4) (1999) 574–608.
[13] J. Zhang, P.D. Olcott, G. Chinn, A.M.K. Foudray, C.S. Levin, Study of the performance of a novel 1 mm resolution dual-panel PET camera design dedicated to breast cancer imaging using Monte Carlo simulation, Med. Phys. 34 (2) (2007) 689–702.